Far-infrared rays control prostate cancer cells *in vitro* and *in vivo*

Hiroki Shima [1], Shingo Yamamoto[1], Jun Qiu[1], Mayumi Shincho[2], Seiichi Hirota[2], Yoshie Yoshikawa[3], Reigetsu Yoshikawa[3] and Tomoko Hashimoto-Tamaoki[3]

1. Department of Urology, Hyogo College of Medicine, Nishinomiya, Japan

2. Department of Surgical Pathology, Hyogo College of Medicine, Nishinomiya, Japan

3. Department of Genetics, Hyogo College of Medicine, Nishinomiya, Japan

Correspondence to: Hiroki Shima [1] Correspondence and requests for materials should be addressed to H.S. (Email: uro-hito@hyo-med.ac.jp)

We introduce a new effective method to control hormone refractory prostate cancer cells by using an activated rubber/resin form (RB), far-infrared ray emitter, with or without sodium butyrate (SB). The growth of three human prostate cancer cell lines (Du145, PC-3 and LNCaP) was suppressed *in vitro* and *vivo* by using RB, and the cells were eradicated with RB + 3 mM SB. G_1 arrest and apoptotic pathway proteins were induced by RB with intensified expressions of apoptosis - related mRNA on cDNA microarray. RB radiates the infra-red rays of the 4 to 25 μm wavelengths to an object which exert a favorable influence on a cancer control. These results may render us a new therapeutic modality in hormone refractory prostate cancer.

Prostate cancer is the most common malignancy in men in the USA, with 218,890 new cases and 27,050 deaths estimated in 2007 [1]. Treatment options for early-stage prostate cancer are well defined, and localized prostate cancer can be cured by several therapeutic strategies. However, the outcome is still disappointing in advanced prostate cancer [2]. A variety of chemotherapeutic approaches, including docetaxel, have been tried to control hormone-refractory prostate cancer, but none are yet fully satisfactory in terms of complete cure, with the least number of side effects [3]. An effective new modality for the treatment of hormone refractory prostate cancer is urgently needed.

Current studies on cancer control have focused on cancer-specific genes and proteins to control cancer [4], with which there are some expectations of cancer control *in vitro* and/or *in vivo* [4, 5]. However, the most difficult issue in studies of cancer control is the cancer itself, since it is already established when it is studied. We know that it constantly changes its own DNA arrangement and increases in size, which leads to the death of the host. Cancer cells also have normal active genes for their survival and growth [6]. On the other hand, genes to suppress cancer growth might become considerably silent during cancer growth [7]. It is also considered that apoptotic pathways in cancer cells are inactivated or weakened [8]. It will be then very effective in cancer control if such an oncogenic environment in a man with cancer whose death pathways of cancer cells become silent is improved by applying a new method to reactivate silent and/or weakened pathways of apoptosis and its related genes. In

order to reactivate these silent genes, we focused on both far-infrared rays and sodium butyrate (SB), natural histone deacetylase inhibitors (HDACi) in human intestine.

Under conditions in which the DNA loop is open widely for SB, and more active movements of molecules in nuclei occur with an increase of the temperature induced by far-infrared rays, various transcription factors have more efficient access to the promoter region of the structural genes.

For this purpose, we chose an activated rubber/resin form made of natural or synthetic rubber/resin (RB) originally applied to a wetsuit, and known to be far-infrared ray emitter. We assessed the ability of this activated form in combination with SB to control human prostate cancer cells such as DU145, PC-3 and LNCaP [9, 10]. Furthermore, we propose a new concept to explain the observed efficacy of RB in the growth control of prostate cancer cells using the Planck and Arrhenius formula [11, 12]. RB increased the temperature by 0.36°C constantly in the area exposed, which resulted in the reactivation of mRNA expression of apoptotic pathways in the prostate cancer cells on cDNA microarray analysis. These phenomenon by RB were confirmed through a set of both *in vitro* and *in vivo* experiments. This could be theoretically brought by the effects of the structure-based substance wave at a frequency of 2.23×10^{33}/s radiated from the molecules by resonance when exposed to far-infrared rays.

Spectral emissivity in the infrared region

Spectral emittance from 4 to 25 μm was close to 100 % (Fig.1a). Transmissivity was Zero (0) at 4000 - 400cm^{-1} (Data not shown). The temperature of the medium increased by 0.36°C (37.32 ± 0.405 *vs* 37.68 ± 0.440, n = 12) by far-infrared rays emitted from RB which were placed up and down outside the culture dish (Fig.1b).

Effects of RB ±SB on prostate cancer cells

We started the following experiments after the cell culture for 3 weeks with or without RB. Since preliminary cDNA microarray of the cancer cells cultured showed incremental increases of mRNA expression from the 1st day to 3ird week (Data not shown). We observed a significant decrease in cell proliferation in DU145, PC-3, and LNCaP cell lines after 8 days of treatment with RB ± SB (Fig.1c). However, each cell line showed a somewhat different response to RB, SB and RB+SB. After 8 days, RB inhibited cell proliferation by 59.2% ($P<0.0001$) in DU145 cells (Fig. 2a and Supplementary Table 1), 56.9% $P<0.0001$) in PC-3 (Fig. 2b and Supplementary Table 1), and 31.5% ($P<0.0001$) in LNCaP cells (Fig. 2c and Supplementary Table 1). Treatment with RB+SB (2 mM) showed a stronger inhibition of cell growth than treatment with 2mM SB alone after 8 days: 4.4–99.1% ($P<0.0001$) in DU145 cells (Fig. 2a and Supplementary Table 1), 27.7–93.4% ($P<0.0001$) in PC-3 cells (Fig. 2b and Supplementary Table 1) and 87.7–100% ($P<0.0001$) in LNCaP cells (Fig. 2c and Supplementary Table 1). The cells (DU145, PC-3 and LNCaP) with RB attachment died in the presence of 3mM SB. These date indicated that hormone-refractory

prostate cancer cells DU145 and PC-3 were significantly suppressed by RB+SB, which had a stronger growth inhibitory effect than that of SB alone.

Human prostate epithelial cells (PrEC) were subjected to the same treatment. After 8 days, 1, 2 and 3 mM SB inhibited cell proliferation by 27.3% ($P<0.01$), 24.0% ($P<0.01$) and 24.3% ($P<0.01$), respectively (Fig. 2d and Supplementary Table 1). Surprisingly, we observed a significantly increase in the number of normal PrEC following RB+SB treatment. Eight days treatment with RB+SB (0, 1, 2 and 3 mM) increased the number of cells by 69.5% ($P<0.01$), 53.6% ($P<0.001$), 50.0% ($P<0.001$) and 192.8% ($P<0.0001$), respectively (Fig. 2d and Supplementary Table 1). These results suggest that RB is not toxic to human PrEC, but SB is toxic to a certain extent. Interestingly, RB increased the number of human PrEC in culture.

Gene expression on cDNA microarray

Expression of mRNA in the presence of RB was recognized from day 1, and increased up to week 3 in the preliminary experiment. Representative results of hierarchical clustering human cDNA (1.2k) microarray analysis after 3 and 4 weeks' exposure of cells to RB is shown in Fig. 3A. RB showed remarkable activation of mRNA in DU145, PC-3 and LNCaP cells after 3 and 4 weeks. In combination of 2 mM SB for 7 days which the culture medium were exposed by RB for 3 weeks, mRNA expression was intensified in the presence of 2 mM SB which the culture medium were not exposed by RB for 3 weeks. mRNA for TNF associated genes related to apoptosis was strongly expressed which was confirmed by RT-PCR (Fig.

3b). Messenger RNA related to MAP kinase and ubiquities pathways were not activated by RB (data not shown).

Effect of RB on the prostate cancer cell cycle

In the cell cycle analysis, RB decreased the percentage of DU145 cells in S phase (Fig. 4a and Supplementary Table 2). The result of laser scanning cytometry indicated a 71% ($P<0.01$) decrease in the S phase fraction of cells when DU145 cells were treated with RB for 4 weeks. SB also inhibited the progression of DU145 cells from G_0/G_1 to S phase; at that time cells are committed to replication. These results indicated that RB induced G_1 arrest. Similar changes were observed in PC-3 and LNCaP cells (Fig. 4a and Supplementary Table 2). The results suggest that inhibition of deregulated cell cycle progression is one of the molecular events associated with selective anticancer efficacy of RB in prostate cancer cells.

The regulatory proteins of the checkpoint of G_1/S such as CDK inhibitors (p21 and p27), CDK2, CDK4 and CDK6 were affected by RB and RB+SB treatment. The results showed that the expression of p21 and p27 was significantly increased in DU145 and PC-3 cells with RB and RB+SB treatment, but not in LNCaP cells. The expression of CDK2 was decreased in LNCaP cells, and the expression of CDK4 was decreased in DU145 and PC-3 cells with RB and RB+SB treatment. The expression of CDK6 was decreased in DU145 and PC-3 cells with RB treatment, but increased by RB+SB (Fig. 5a). These results suggested that RB and RB+SB caused G_1 arrest by up-regulation of p21 and p27 expression in DU145 and PC-3 cells, and inhibition of CDK2, CDK4 or CDK6 in all prostate cancer cells.

RB ± SB induce apoptosis in prostate cancer cells

After treatment of prostate cancer cells with RB for 4 weeks, apoptotic cells were detected by laser scanning cytometry. DU145, PC-3 and LNCaP cells treated with RB for 4 weeks exhibited a sub-G_1 peak in laser scanning cytometry (Fig. 4a). Cell morphology under laser scanning microscopy showed condensed and fragmented nuclei in these prostate cancer cells (Fig. 4b). The results showed that RB induced apoptosis in all three prostate cancer cell lines.

Several proteins, including poly (ADP-ribose) polymerase (PARP), play an important role in the condensation and degradation of cell chromatin through apoptotic death. The cleavage of PARP protein is considered as an important biomarker of apoptosis. RB treatment caused a moderate degradation of PARP protein in LNCaP cells. RB+SB treatment caused significant degradation of PARP protein in all prostate cancer cells, and its degradation was stronger than that with SB treatment (Fig. 5b). These results suggested that RB and RB+SB induced apoptosis of prostate cancer cells by activating PARP cleavage.

We also analyzed the level of caspase-3, which is known to be the main effector caspase in most mammalian cells, following 1week treatment with SB. We showed that the expression of procaspase-3 was significantly down-regulated in DU145, PC-3 and LNCaP cells undergoing apoptosis during treatment with RB+SB, and the degradation was stronger than that with SB treatment alone. Expression of procaspase-3 was also significantly down-regulated in LNCaP cells and slightly

down-regulated in PC-3 cells during treatment with RB for 4 weeks (Fig. 5b). These results suggested that RB- and RB+SB-induced apoptosis of prostate cancer cells were mediated through caspase-3.

RB treatment caused significant induction of Bcl-2 and Bcl-xL expression. Furthermore, expression of Bcl-2 was significantly decreased in LNCaP cells, Bcl-xL expression was moderately decreased in PC-3 and LNCaP cells, and Bax expression was not significantly changed in PC-3 and LNCaP cells (Fig, 5b). In DU145 cells, Western blot analysis did not reveal the presence of Bcl-2 or Bax. Treatment of cells with RB+SB significantly induced the expression of Bcl-2 in PC-3 cells, and the degradation was stronger than that with SB treatment. These data suggested that RB and RB+SB induced apoptosis of PC-3 and LNCaP cells through the Bcl-2- and Bcl-xL-mediated apoptosis pathway.

As shown in Fig. 5b, DU145 and LNCaP cells treated with RB+SB exhibited a significant increase in the expression of TRADD and FADD, death adaptor proteins, and the increase was greater than that with SB treatment alone. DU145 cells treated with RB also exhibited a significant increase in the expression of Fas death receptor protein. These data suggested that RB induced apoptosis of DU145 cells through a Fas-mediated pathway. RB+SB also induced apoptosis in DU145 and LNCaP cells through a Fas-mediated pathway.

Apoptotic effect of RB on tumor growth *in vivo*

We examined the inhibitory effects of RB to the growth of prostate cancer cells

transplanted into nude mice. The growth curves for prostate cancer xenografts are shown in Figure 6 a-c. There was a significant decrease of 16.7% (*$p<0.05$) in tumor volume on the 70^{th} day in DU-145, 53.1% (*$p<0.05$) on the 74^{th} day in PC-3, and 67.1% (*$p<0.05$) on the 15^{th} day in LNCaP as a result of RB treatment. The result showed that RB had an inhibitory effect *in vivo* against proliferation of human prostate cancer cells.

Apoptosis was demonstrated by the TUNEL reaction in the xenografts mice tissues. Apoptosis was clearly shown by scattered TUNEL-positive cells in sections of all prostate cancer tissue when the xenografts mice were exposed to RB, but not shown without RB exposure (Fig 6d).

Discussion

The response of hormone-refractory prostate cancer to chemotherapy remains modest, necessitating the search for new forms of treatment to improve the prognosis. This study is believed to be the first to show that exposure to RB was effective at inhibiting the growth of human prostate cancer cells (DU145, PC-3 and LNCaP), and RB+SB at low concentration induced complete eradication of these cancer cells *in vitro*. In addition tumor growth of all three prostate cancer cells was also significantly suppressed *in vivo*. Our data also suggest that RB-induced growth inhibition of cancer cells was associated with strong G1 phase arrest, by increasing p21 expression, which resulted in CDK2, CDK4 or CDK6 down-regulation. The apoptosis induced by RB and RB+SB is thought to be mediated by a Bcl-2 and Fas signaling pathway.

The genes involved in the suppression of cancer growth are more or less inactivated in patients with cancer, which results in oncogene–activation in these patients [7]. This condition may be induced by the gene mutation, but usually it explains approximately 10% of all cancers. The most problem of cancer research is in the object of research, since all kinds of scientific analysis including gene mutation in cancer cells is done after cancer is established. The total number of genes in humans is 20 000–25 000 [13], but the number of active genes decreases with aging [14].

It is well known that histone acetyl transferase opens up the space of histones that allows specific transcription factors to bind the promoter to activate the structure gene, this will produce proteins available for keeping a man in healthy homeostasis under normal condition [15]. If cells are exposed to HDACis, it may be that the genes

remain active, which may give more opportunity for silent genes to be reactivated. In addition, the increase of temperature at a certain degree may give more chances of the transcription factors to bind the promoters by increasing rate of molecular collisions according to Arrhenius plot resulting in reactivation of the silent and/or inactive genes.

Taking into consideration that various kinds of gene activation in the cDNA microarray clustering analysis, and the inhibition of cancer growth observed by the exposure of prostate cancer cells to RB, it appears that far-infrared rays play an important role in the gene activation.

The reason why RB has such high emittance of far-infrared rays is due to many closed cells exist in the RB (20 to 30 cells / mm^2). Since RB has much larger development area and can receive many infrared rays e.g. from the sun and heat - generating objects.

When a spectral emittance was measured, it was found that RB has a spectral emittance close to “1 (100%)” in the area from 4 μm to 25 μm, which is equal to a spectral emittance of virtual black body similar to a sunspot.

The temperature difference after exposure of the culture medium to RB is only 0.36°C. The main wavelength of far-infrared rays emitted form RB is 4–25 μm. Calculating from the velocity of light, the frequency of far-infrared rays at 4 - 25 μm is $1.2 \sim 7.5 \times 10^{13}$, which is not a sufficient energy level to increase the temperature of the culture medium by 0.36°C. The energy needed to increase the temperature of 1 g water by 1°C is 4.184 J · s. Therefore, it will be 1.48 J · s in order to increase the

temperature by 0.36°C. From Planck's formula, the frequency of the wave to raise the temperature by 0.36°C must be 2.23×10^{33} /s [16]. To explain this discrepancy between the two energy levels, it might be assumed that there exists the structure-based substance wave at frequency of 2.23×10^{33} /s, which is probably generated from molecules by resonance in culture media and cells when they are exposed to far-infrared rays. The increased temperature caused by constant exposure to far-infrared rays increases the collision rate among molecules, according to the equation of the Arrhenius plot[17]. The increase of collision rate may be small, but estimating the tremendous numbers of the combinations of molecules in the cells, the collisions may be significant to activate interrelation among the molecules necessary for activation of the silent genes, which induced mRNA re-expression and re-activation of apoptotic pathway as were shown in the Figure 3a & b. Acetyl transferase alters chromatin structure and dynamically affects transcription regulation. HDACis keep an altered chromatin structure and are highly effective in up-regulating suppressor gene expression. The increased temperature induced by far-infrared rays may lead to up-regulation of suppressor and/or apoptotic genes, especially in the presence of HDACi in cancer cells. In this study, treatment of cells with RB+SB significantly induced expression of Bcl-2 and Bcl-XL, and considerably increased expression of TRADD and FADD proteins.

Apoptosis plays an important role in the renewal of the normal and neoplastic prostatic epithelium, and reduced apoptosis is associated with the progression of locally invasive prostate cancers to metastatic disease [18, 19]. Restoring apoptosis has

been suggested as a possible therapeutic strategy, therefore, a great deal of research has been devoted to understanding the abnormalities in the cellular machinery that cause resistance to apoptosis in prostate cancer cells [19]. Increasing evidence indicates that impaired ability to undergo apoptosis plays an important role in the evolution from androgen-dependent to androgen-independent prostate cancer, as well as drug resistance [20]. Thus, much effort is being directed toward finding ways to increase apoptosis in prostate cancer. In this study, we showed that RB and RB+SB induced apoptosis. In addition, it is very important that RB did not harm the growth of normal prostate epithelium, and rather increased the number of normal prostate epithelial cell in the presence of SB, otherwise growth was suppressed by SB.

This is believed to be the first report of the biological action of RB in prostate cancer cell lines. We demonstrated that prostate cancer cell lines were sensitive to RB and RB+SB *in vitro* and *in vivo*. Two distinct signaling pathways were involved in RB-mediated cell growth arrest and induction of apoptosis. These results present a new therapeutic modality, especially in hormone-refractory prostate cancer, and theoretically RB might be helpful to control various kinds of cancer.

Methods Summary

The activated form (RB) made of natural or synthetic rubber/resin was obtained from Yamamoto (Osaka, Japan) (Fig. 1d). RB consisted of rubber, lime stone and titanium metal powder in a honeycomb structure comprised of micron-sized cells, and had the ability to radiate far-infrared rays (4–25 μm) and maintain body temperature. The spectral emissivity 2500 cm^{-1} – 400 cm^{-1} (4 μm – 25 μm) was measured at the measuring temperature 90°C, Discrimination 8 cm^{-1} and the integrated 200 times testing by SIMADZ Fourier transform infrared spectrophtometer FTIR - 4300 (Figure 1d). Spectral Transmission of RB in the infrared region was measured by SHIMADZU infrared spectrophotometer IR-470.

The DU145, PC-3 and LNCaP cell lines were maintained in minimum essential medium, F-12K medium and RPMI medium. The temperature of the culture medium that was exposed to RB was measured in an atmosphere of 5% CO_2 at 37°C by a digital thermometer, after the door of the incubator was kept closed for 30 min.

For determining cell proliferation, viable cell numbers were counted using the Cell Proliferation Kit II (Roche Diagnostics, Mannheim, Germany) based on the XTT assay [21].

Hierarchical clustering was applied to both axes using the unweighted pair-group method, with the arithmetic average as implemented in the program GeneSpring5.1 (Agilent Technologies, Santa Clara, CA, USA). Messenger RNA for TNF associated genes related to apoptosis which showed strong signal intensity were confirmed by RT-PCR independently [22].

Cell cycle and apoptosis analysis were examined under a laser scanning microscope (Olympus BX51; Olympus Optics, Tokyo, Japan) [23]. Effect of RB and RB+SB on expression of apoptotic proteins was performed with Western blotting.

To explore the relevance of our findings *in vivo*, we examined the inhibitory effects of RB by tumor xenograft studies, apoptosis was demonstrated by the TUNEL reaction in the xenografts mice tissues.

References

1. Jemal, A. et al. Cancer statistics, 2007. *CA Cancer J Clin* **57**, 43-66 (2007).
2. Yagoda, A. & Petrylak, D. Cytotoxic chemotherapy for advanced hormone-resistant prostate cancer. *Cancer* **71**, 1098-1109 (1993).
3. Petrylak, D.P. Docetaxel-based chemotherapy trials in androgen-independent prostate cancer: first demonstration of a survival benefit. *Curr Oncol Rep* **7**, 205-206 (2005).
4. Prosperi, J.R. & Robertson, F.M. Cyclooxygenase-2 directly regulates gene expression of P450 Cyp19 aromatase promoter regions pII, pI.3 and pI.7 and estradiol production in human breast tumor cells. *Prostaglandins Other Lipid Mediat* **81**, 55-70 (2006).
5. Schoensiegel, F. et al. MIA (melanoma inhibitory activity) promoter mediated tissue-specific suicide gene therapy of malignant melanoma. *Cancer Gene Ther* **11**, 408-418 (2004).
6. Rao, M.K., Maiti, S., Ananthaswamy, H.N. & Wilkinson, M.F. A highly active homeobox gene promoter regulated by Ets and Sp1 family members in normal granulosa cells and diverse tumor cell types. *J Biol Chem* **277**, 26036-26045 (2002).
7. Frebourg, T. et al. Germ-line mutations of the p53 tumor suppressor gene in patients with high risk for cancer inactivate the p53 protein. *Proc Natl Acad Sci U S A* **89**, 6413-6417 (1992).
8. Karam, J.A., Lotan, Y., Ashfaq, R., Sagalowsky, A.I. & Shariat, S.F. Survivin expression in patients with non-muscle-invasive urothelial cell carcinoma of the bladder. *Urology* **70**, 482-486 (2007).
9. Horoszewicz, J.S. et al. The LNCaP cell line--a new model for studies on human prostatic carcinoma. *Prog Clin Biol Res* **37**, 115-132 (1980).
10. Kaighn, M.E., Narayan, K.S., Ohnuki, Y., Lechner, J.F. & Jones, L.W. Establishment and characterization of a human prostatic carcinoma cell line (PC-3). *Invest Urol* **17**, 16-23 (1979).
11. Roccatano, D., Sahoo, H., Zacharias, M. & Nau, W.M. Temperature dependence of looping rates in a short peptide. *J Phys Chem B* **111**, 2639-2646 (2007).
12. Binaschi, M., Zunino, F. & Capranico, G. Mechanism of action of DNA topoisomerase inhibitors. *Stem Cells* **13**, 369-379 (1995).

13. Finishing the euchromatic sequence of the human genome. *Nature* **431**, 931-945 (2004).
14. Burzynski, S.R. Aging: gene silencing or gene activation? *Med Hypotheses* **64**, 201-208 (2005).
15. Struhl, K. Histone acetylation and transcriptional regulatory mechanisms. *Genes Dev* **12**, 599-606 (1998).
16. Planck, M. Ueber das Gesetz der Energieverteilung im Normalspectrum; von Max Planck. *Ann. d. Phys.* **4**, 553-563 (1900).
17. Arrenhius, S. Uber die Reaktionsgeschwindigkeit bei der Inversion von Rohrzucher durch Sauren. *Z. Phys, Chem.* **4**, 226 (1889).
18. Bruckheimer, E.M. & Kyprianou, N. Apoptosis in prostate carcinogenesis. A growth regulator and a therapeutic target. *Cell Tissue Res* **301**, 153-162 (2000).
19. Peehl, D.M. Primary cell cultures as models of prostate cancer development. *Endocr Relat Cancer* **12**, 19-47 (2005).
20. Gurumurthy, S., Vasudevan, K.M. & Rangnekar, V.M. Regulation of apoptosis in prostate cancer. *Cancer Metastasis Rev* **20**, 225-243 (2001).
21. Maier, S. et al. Tributyrin induces differentiation, growth arrest and apoptosis in androgen-sensitive and androgen-resistant human prostate cancer cell lines. *Int J Cancer* **88**, 245-251 (2000).
22. Ito, Y. et al. Co-expression of matriptase and N-acetylglucosaminyltransferase V in thyroid cancer tissues--its possible role in prolonged stability in vivo by aberrant glycosylation. *Glycobiology* **16**, 368-374 (2006).
23. Shibata, M.A., Ito, Y., Morimoto, J. & Otsuki, Y. Lovastatin inhibits tumor growth and lung metastasis in mouse mammary carcinoma model: a p53-independent mitochondrial-mediated apoptotic mechanism. *Carcinogenesis* **25**, 1887-1898 (2004).
24. Li, H., Cao, H.F., Li, Y., Zhu, M.L. & Wan, J. Changes in gene-expression profiles of colon carcinoma cells induced by wild type K-ras2. *World J Gastroenterol* **13**, 4620-4625 (2007).
25. Bedner, E., Li, X., Gorczyca, W., Melamed, M.R. & Darzynkiewicz, Z. Analysis of apoptosis by laser scanning cytometry. *Cytometry* **35**, 181-195 (1999).
26. Klisovic, D.D. et al. Depsipeptide (FR901228) inhibits proliferation and induces apoptosis in primary and metastatic human uveal melanoma cell lines. *Invest*

Ophthalmol Vis Sci **44**, 2390-2398 (2003).

27. Wiese, L., Kurtzhals, J.A. & Penkowa, M. Neuronal apoptosis, metallothionein expression and proinflammatory responses during cerebral malaria in mice. *Exp Neurol* **200**, 216-226 (2006).

Acknowledgements We thank greatly Hitoshi Amano, Physicist, Dr. Sc. for his support to our theory, Taiki Tamaoki Ph.D. for the critical comments, Akiko Yamasaki, and Chihiro Satoh for their technical assistance.

Author Contributions The experiments were conceived and designed by H.S. Experiments were performed by H.S., J.Q., M.S., and Y.Y. Immunohistochemistry of mice samples was conducted and investigated by M.S., and S.H. Experiments on cDNA microarray were performed by Y.Y., Y.R., and T.H.T. Data were analysed by H.S., S.Y., and J.Q. The paper was written by H.S., S.Y., and J.Q.

Author Information Reprints and permissions information is available at www.nature.com/reprints. The authors declare no competing financial interests. Correspondence and requests for materials should be addressed to H.S. (uro-hito@hyo-med.ac.jp)

Table 1 | Effect of RB, SB and RB + SB on the growth of cells

	Alive cell number (%) on the 8th day							
	DU145		PC-3		LNCaP		PrEC	
SB	RB (-)	RB (+)	RB (-)	RB (+)	RB (-)	RB (+)	RB (-)	RB (+)
0 mM	549.6 ± 0.4	224.3 ± 5.3*	859.9 ± 45.9	370.8 ± 69.9*	401.4 ± 23.4	274.8 ± 18.2*	100.0 ± 9.7	169.2 ± 18.3+
1 mM	546.4 ± 0.1	56.8 ± 9.9*	847.0 ± 29.9	204.9 ± 44.6*	146.9 ± 10.1	22.0 ± 10.6*	73.2 ± 7.9+	111.6 ± 17.9#
2 mM	525.4 ± 10.5	4.8 ± 0.4*	622.1 ± 96.9	38.0 ± 13.2*	49.2 ± 4.7	0.0 ± 0.0*	75.7 ± 7.8+	111.4 ± 12.7#
3 mM	100.0 ± 15.0	0.0 ± 0.0*	301.4 ± 47.8	0.0 ± 0.0*	6.8 ± 2.2	0.0 ± 0.0*	76.8 ± 8.1+	224.9 ± 16.9*

Data shown are the mean ± SD (%). +, $p < 0.01$; #, $p < 0.001$; *, $p < 0.0001$. PrEC: prostate epithelial cell

Table 2 | Effect of RB treatment on cell cycle and apoptosis

Cell line	RB	G0	G1	S	G2	M	sub-G1
DU145	–	0.3 ± 0.2	56.1 ± 1.8	15.4 ± 1.5	14.9 ± 0.9	0.9 ± 0.5	0.5 ± 0.1
	+	1.4 ± 0.5	67.5 ± 3.1+	1.5 ± 1.3#	9.8 ± 1.9	0.6 ± 0.2	6.4 ± 0.4*
PC-3	–	12.4 ± 1.3	54.9 ± 1.2	6.9 ± 0.2	6.9 ± 1.1	1.4 ± 0.1	0.7 ± 0.4
	+	2.3 ± 0.2	82.8 ± 1.9*	1.4 ± 0.2*	2.2 ± 0.4	0.2 ± 0.1	6.2 ± 0.2*
LNCaP	–	0.4 ± 0.2	59.3 ± 1.4	16.1 ± 0.7	12.5 ± 1.5	0.9 ± 0.3	0.1 ± 0.1
	+	0.8 ± 0.8	63.3 ± 2.3	12.7 ± 1.3ϕ	11.3 ± 1.5	0.9 ± 0.7	3.1 ± 0.2*

Data shown are the mean ± SD (%). ϕ, $p < 0.05$; +, $p < 0.01$; #, $p < 0.001$; *, $p < 0.0001$

Table 1 | Effect of RB, SB and RB + SB on the growth of prostate cancer cell lines and human prostate epithelial cells

Table 2 | Effect of RB treatment on cell cycle and apoptosis in DU145, PC-3, and LNCaP cells

Figure legends

Figure 1 | The spectral emissivity and transmissivity of RB, and experimental design. (**a**) The spectral emissivity (4 μm – 25 μm) was measured at the measuring temperature 90°C. The respective spectrum of the spectral emissivity of a dummy blackbody as well as of RB are shown. Conversion formula is shown as Xμm =10000/Y cm^{-1} (for example: 10000/400 cm^{-1}=25 μm). Spectral Transmission of RB in the infrared region was measured, and transmissivity was Zero (0) at 4000 - 400 cm^{-1} (Data not shown). (**b**) Prostate cancer cells were cultured in 10-cm dishes which were exposed to RB whose silver color side toward cells. (**c**) Prostate cancer cells were cultured with or without RB for 3 weeks, and SB was then added to the culture medium at 2 mM for 1 week. (**d**) Activated form of RB with a honeycomb structure comprised of micron-sized cells (20-30/mm^3) inside has the ability to radiate far-infrared rays (4–25 μm).

Figure 2 | **Effects of RB, SB and RB+SB on the growth of prostate cancer cell lines and human prostate epithelial cells.** (**a**) DU145, (**b**) PC-3, (**c**) LNCaP, and (**d**) human prostate epithelial cells. DU145, PC-3, LNCaP and human prostate epithelial cells were treated with RB with or without 0.2% PBS (–) or 1, 2 and 3 mM SB for 8 days; cells were counted after 2, 5 and 8 days by XTT assay. Data from three independent experiments are shown as means ± SD. $^{+}P<0.01$, $^{\#}P<0.001$, $^{*}P<0.0001$.

Figure 3 | **Hierarchical clustering analysis in treatment of prostate cancer cell lines by RB, SB and RB+SB.** (**a**) Gene expression profile. Representative results of hierarchical clustering human cDNA (1.2k) microarray analysis after 3 and 4 weeks exposure to RB are shown. RB showed remarkable activation of mRNA in DU145, PC-3, and LNCaP cells. In combination of 2 mM SB for 7 days which the culture media were exposed by RB for 3 weeks, mRNA expressions were intensified in the presence of 2 mM SB which the culture media were exposed by RB for 3 weeks. (**b**) mRNA of TNF associated genes was activated in the presence of RB for 3 weeks. Each row represents the mean of signal log ratios using a color-code scale. Red represents expression that was two-fold greater than the reference value; pink represents expression that was 1.4-fold greater than reference; and green represents expression that was 0.5-fold less than reference.

Figure 4 | **Effect of RB on the cell cycle and apoptosis in prostate cancer cell lines.** DU145, PC-3, and LNCaP cells were treated with RB for 7 days and stained for nuclear DNA with propidium iodide (PI). (**a**) The intensity of PI staining was analyzed with the use of a microscope-based multiparameter laser scanning cytometer. 1, G_0; 2, G_1; 3, S; 4, G_2; 5, M; 6, apoptosis (**b**) Apoptosis (arrow) induced by RB was observed by laser scanning microscopy. Cancer cells were fragmented.

Figure 5 | **Effect of RB and RB+SB on the expression of cell cycle regulators** (**a**) **and apoptosis-associated gene expression** (**b**). The

expression of p21, p27, CDK2, CDK4, CDK6, Fas, FADD, TRADD, Bcl-2, Bcl-xL, Bax, procaspse-3 and PARP were determined by Western blotting. Equal loading (30 μg) was confirmed by stripping immunoblots and reprobing them for β-actin. The experiment was independently repeated three times with similar results.

.

Figure 6 | **Inhibition of prostate cancer tumor growth and apoptosis by RB in vivo.** (**a-c**) RB effects on tumor volumes *in vivo*: Tumor volumes are chronogically shown in RB-treated and – untreated xenografts as described in methods. Each column shows the mean ± S.E.M. of tumor volumes measured in 4 xenografts mice. There was a significant decrease of 16.7% (*$p<0.05$) in tumor volume on the 70^{th} day in DU-145, 53.1% (*$p<0.05$) on the 74^{th} day in PC-3, and 67.1% (*$p<0.05$) on the 15^{th} day in LNCaP as a result of RB treatment. (**d**) Representative micrograph of DNA end-labelling (TUNEL) of tissue sections from mice by RB (+) and RB (-) groups. TUNEL labelling of DU145, PC-3 and LNCaP sections from RB-treated mouse reveals positive staining and propidium iodide - detected DNA strand break (arrow). Magnification ×400. Neither TUNEL-positive nor DNA strand breaks cells were observed in cancer tissue sections when they were not exposed to RB. Magnification ×400.

a

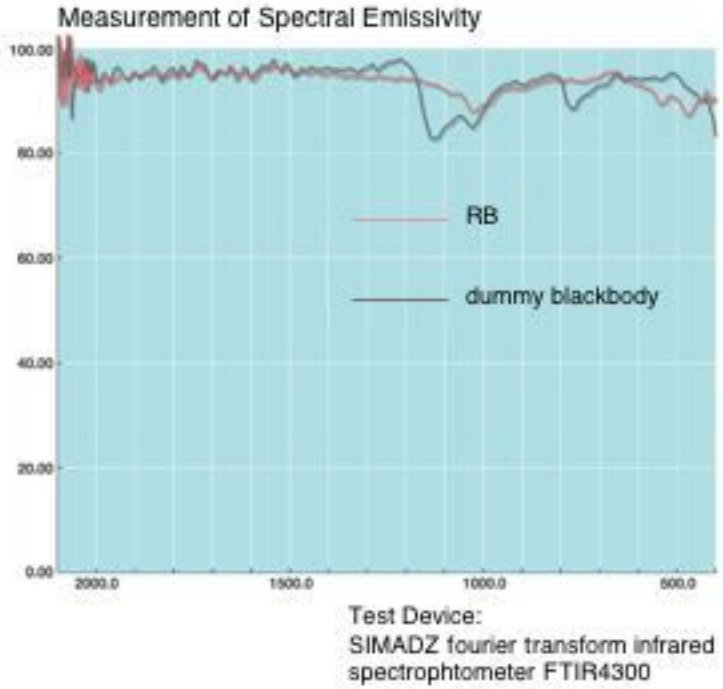

Test Device:
SIMADZ fourier transform infrared spectrophtometer FTIR4300

b

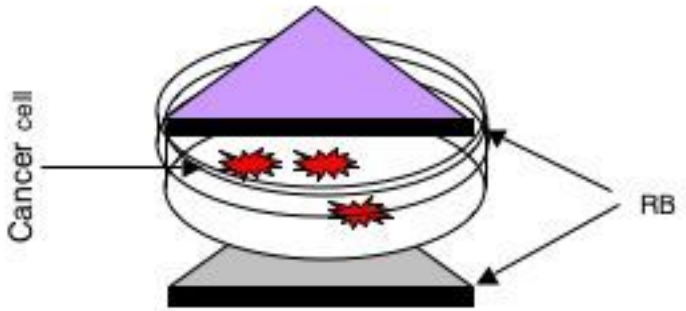

c

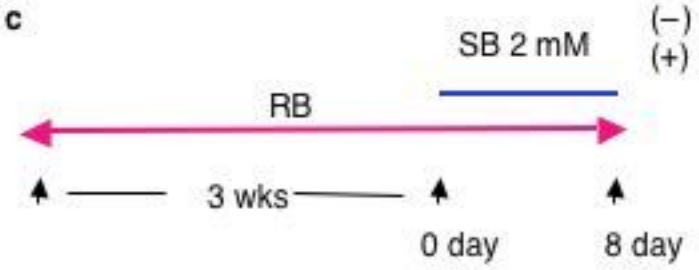

d

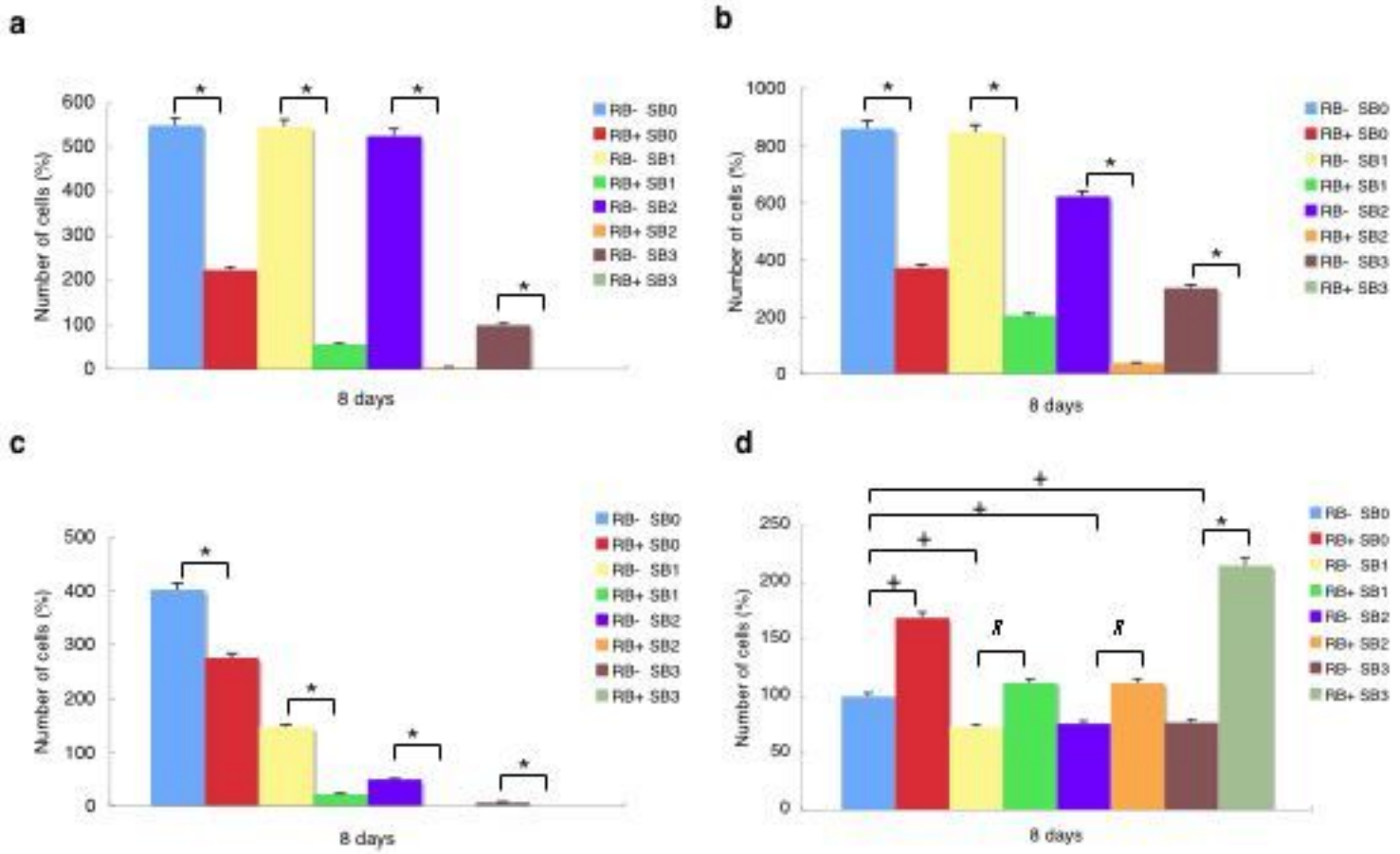
a
b
c
d
Number of cells (%)
8 days
RB- SB0
RB+ SB0
RB- SB1
RB+ SB1
RB- SB2
RB+ SB2
RB- SB3
RB+ SB3

a

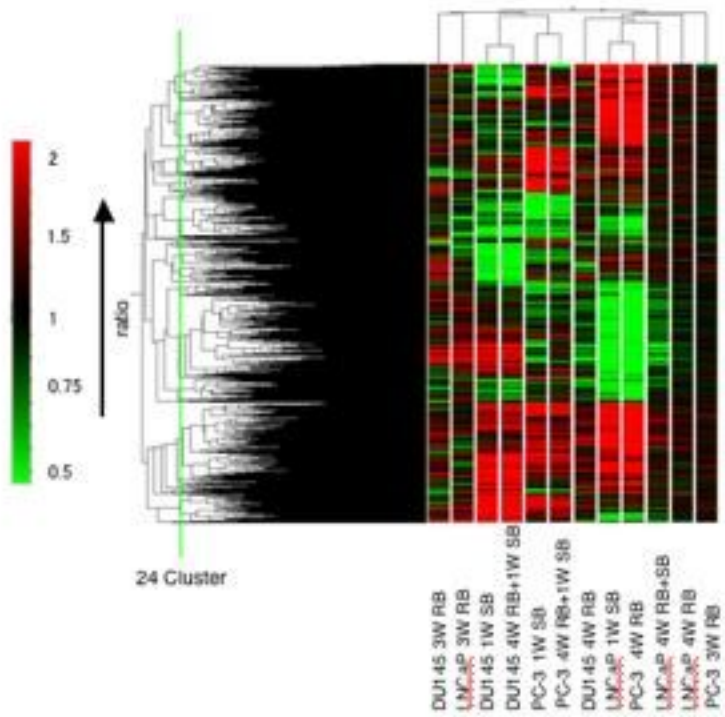

b

Analysis of hierarchical clustering: TNF associated gene expression
(red ≥ 2 folds, pink ≥1.4 green ≤ 0.5)

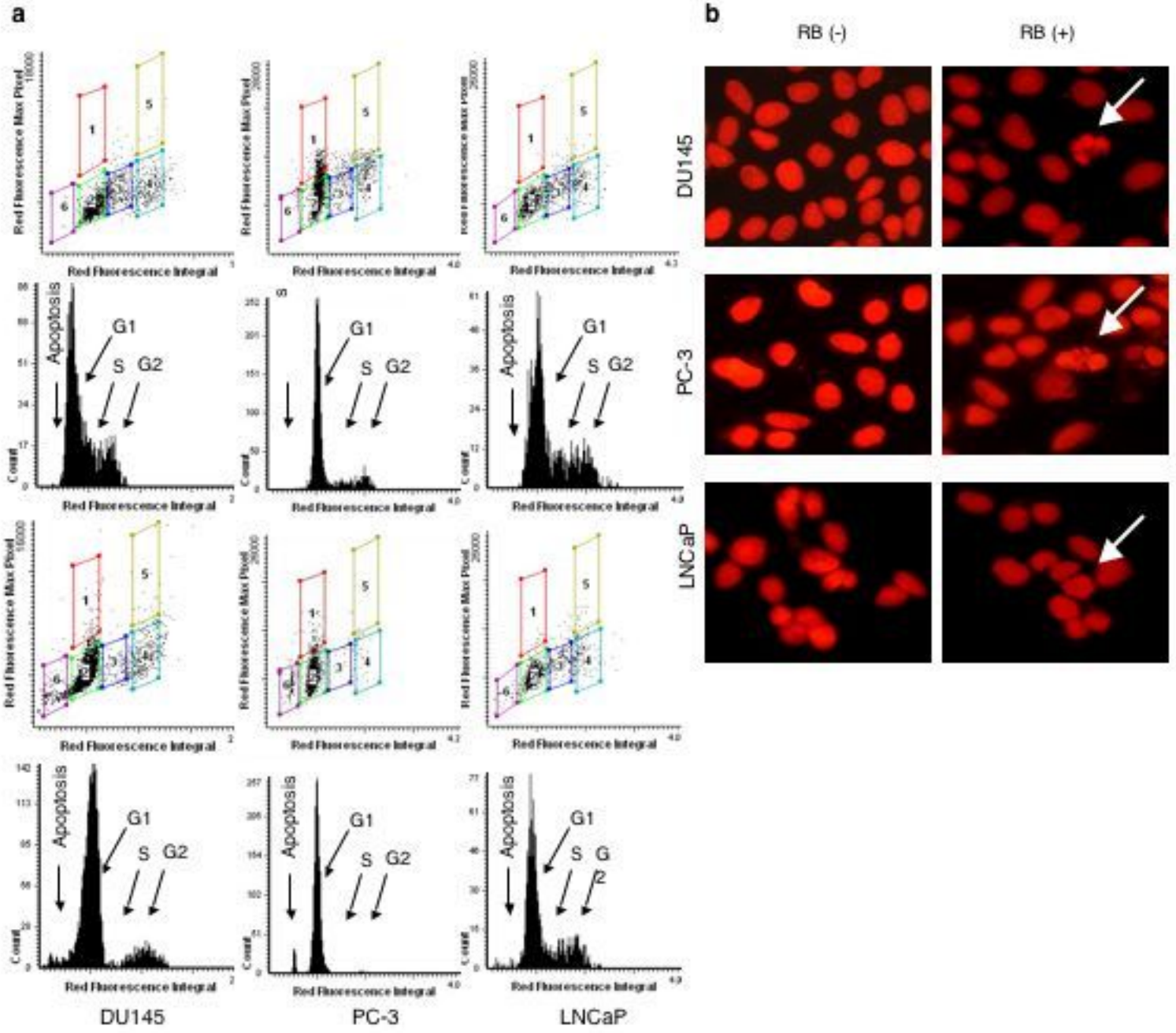
a
b
RB (-)
RB (+)
DU145
PC-3
LNCaP
Red Fluorescence Max Pixel
Red Fluorescence Integral
Count
Apoptosis
G1
S
G2
1
2
3
4
5
6

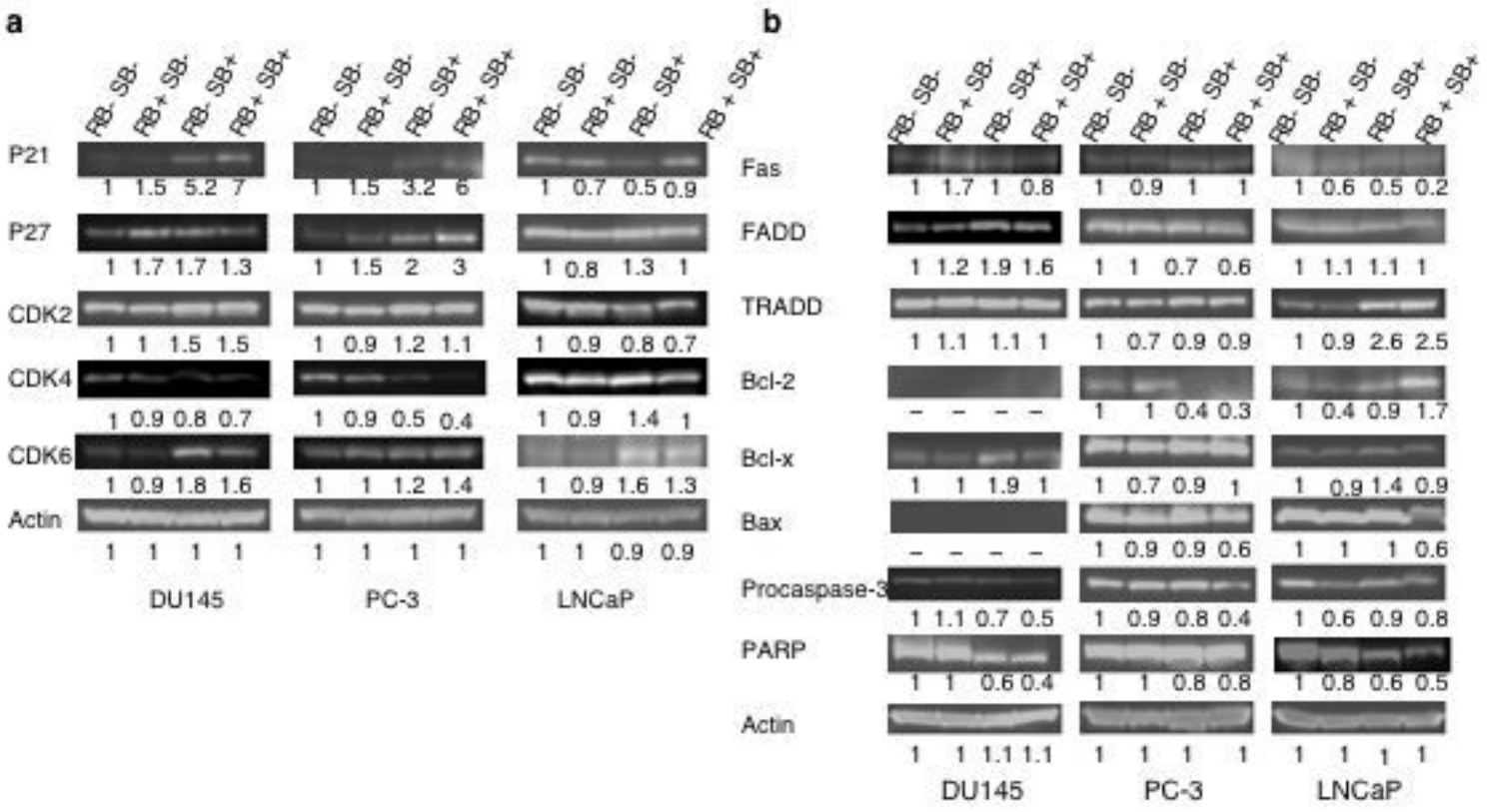
a
RB- SB-
RB+ SB-
RB- SB+
RB+ SB+
P21
1 1.5 5.2 7
1 1.5 3.2 6
1 0.7 0.5 0.9
P27
1 1.7 1.7 1.3
1 1.5 2 3
1 0.8 1.3 1
CDK2
1 1 1.5 1.5
1 0.9 1.2 1.1
1 0.9 0.8 0.7
CDK4
1 0.9 0.8 0.7
1 0.9 0.5 0.4
1 0.9 1.4 1
CDK6
1 0.9 1.8 1.6
1 1 1.2 1.4
1 0.9 1.6 1.3
Actin
1 1 1 1
1 1 1 1
1 1 0.9 0.9
DU145
PC-3
LNCaP
b
RB- SB-
RB+ SB-
RB- SB+
RB+ SB+
Fas
1 1.7 1 0.8
1 0.9 1 1
1 0.6 0.5 0.2
FADD
1 1.2 1.9 1.6
1 1 0.7 0.6
1 1.1 1.1 1
TRADD
1 1.1 1.1 1
1 0.7 0.9 0.9
1 0.9 2.6 2.5
Bcl-2
– – – –
1 1 0.4 0.3
1 0.4 0.9 1.7
Bcl-x
1 1 1.9 1
1 0.7 0.9 1
1 0.9 1.4 0.9
Bax
– – – –
1 0.9 0.9 0.6
1 1 1 0.6
Procaspase-3
1 1.1 0.7 0.5
1 0.9 0.8 0.4
1 0.6 0.9 0.8
PARP
1 1 0.6 0.4
1 1 0.8 0.8
1 0.8 0.6 0.5
Actin
1 1 1.1 1.1
1 1 1 1
1 1 1 1
DU145
PC-3
LNCaP

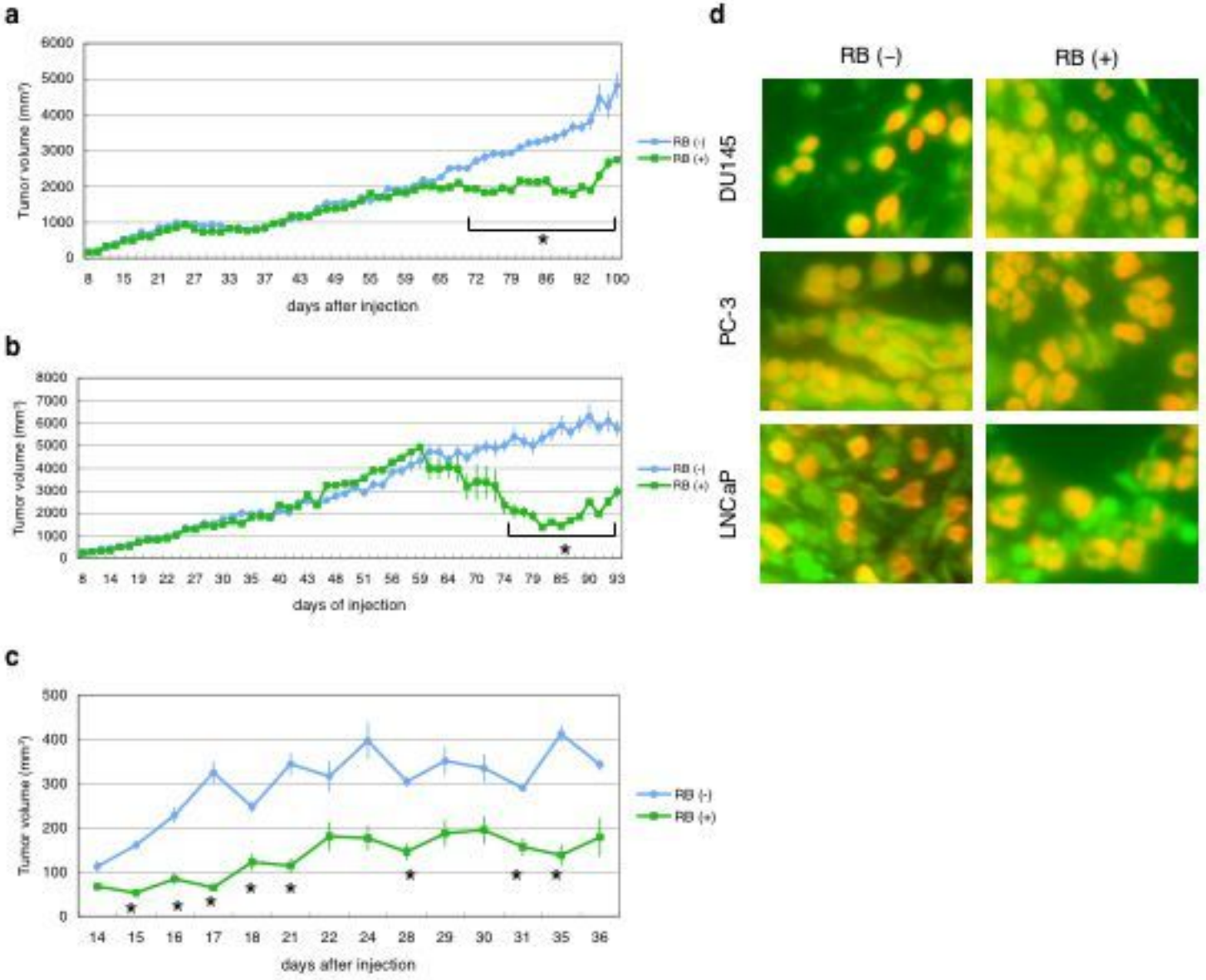
a
Tumor volume (mm³)
6000
5000
4000
3000
2000
1000
0
8 15 21 27 33 37 43 49 55 59 65 72 79 86 92 100
days after injection
RB (-)
RB (+)
b
Tumor volume (mm³)
8000
7000
6000
5000
4000
3000
2000
1000
0
8 14 19 22 27 30 35 40 43 48 51 56 59 64 70 74 79 85 90 93
days of injection
RB (-)
RB (+)
c
Tumor volume (mm³)
500
400
300
200
100
0
14 15 16 17 18 21 22 24 28 29 30 31 35 36
days after injection
RB (-)
RB (+)
d
RB (–)
RB (+)
DU145
PC-3
LNCaP